Dual observations of interplanetary shocks associated with stream interaction regions

E. Aguilar-Rodriguez,[1] X. Blanco-Cano,[2] C. T. Russell,[3] J. G. Luhmann,[4] L. K. Jian,[3] and J. C. Ramírez Vélez[5]

Received 11 February 2011; revised 17 October 2011; accepted 1 November 2011; published 31 December 2011.

[1] We investigate the characteristics of 9 interplanetary shocks associated with stream interaction regions observed by both STEREO-A and STEREO-B spacecraft during the years 2007–2008. Interplanetary shocks modify the plasma both upstream and downstream of the front shock. As they propagate, interplanetary shocks encounter solar wind with different characteristics (density, velocity) and different orientations of ambient magnetic field relative to the shock normal. Thus, it is interesting to compare dual observations of stream interaction shocks at the locations of the two spacecraft to determine the role of these parameters in controlling both the structure at the shock but also in the regions upstream and downstream from the shock. The range of shock normal angle (Θ_{Bn}) values observed by spacecraft covered the range from ∼20° to ∼81°. The largest difference in Θ_{Bn} for the same shock observed at two different longitudinal locations was ∼39°. The shock magnetosonic Mach numbers covered the range of ∼1.1 to ∼2.2, having a largest change for the same shock of ∼0.9. The jump in the field magnitude, i.e., the ratio of downstream magnetic field intensity to upstream magnetic field intensity (B_d/B_u), ranged from ∼1.1 to ∼2.25. The largest difference in the jump in field magnitude for the same shock at two different locations was ∼0.72. These variations with longitude of shock properties observed with the STEREO dual mission show the non-homogeneous character of the plasma in the heliosphere, and they need to be taken into account to understand in detail how these shocks modify the solar wind, and affect the acceleration processes of energetic particles in the solar wind.

Citation: Aguilar-Rodriguez, E., X. Blanco-Cano, C. T. Russell, J. G. Luhmann, L. K. Jian, and J. C. Ramírez Vélez (2011), Dual observations of interplanetary shocks associated with stream interaction regions, *J. Geophys. Res.*, *116*, A12109, doi:10.1029/2011JA016559.

1. Introduction

[2] One of the first recognized phenomena of solar wind dynamics was the interaction between solar wind streams propagating with different velocities. Fast streams originate in coronal holes [*Krieger et al.*, 1973] and slow streams arise in the streamer belt [*Feldman et al.*, 1981; *Gosling et al.*, 1981] from both the edges of coronal holes [e.g., *Arge and Pizzo*, 2000] and the cusps of coronal streamers [*Wang et al.*, 2000; *Sheeley et al.*, 2001]. When a fast solar wind stream overtakes a slower one, it forms a region where the density and temperature are enhanced as the slow solar wind is compressed and accelerated. This interaction creates a pressure ridge between the two streams, slowing down the fast stream, deflecting it, and speeding up the slow stream and deflecting it. As the streams move outward from the Sun the velocity of the fast compressional mode drops because of the decreasing magnetic field and the change in velocity across the discontinuity becomes larger than the fast mode velocity and a shock can form. Eventually the change in velocity is great enough for two shocks, forward and reverse to form [see, e.g., *Blanco-Cano*, 2010, and references therein]. When the sources of fast solar wind i.e. coronal holes are nearly time-stationary and recur every 27 days on successive solar rotations, the stream interaction regions (SIRs) are known as corotating interaction regions, or CIRs [*Gosling et al.*, 2001]. However, some SIRs do not persist as long as a solar rotation and are not seen 27 days later. It is natural to believe therefore that CIRs are more time-stationary than SIRs but studies with STEREO-A and STEREO-B and intercomparisons with models show that

[1]Unidad Michoacan, Instituto de Geofisica, Universidad Nacional Autonoma de Mexico, Morelia, Mexico.
[2]Instituto de Geofisica, Universidad Nacional Autonoma de Mexico, Mexico City, Mexico.
[3]Institute of Geophysics and Planetary Physics, University of California, Los Angeles, California, USA.
[4]Space Sciences Laboratory, University of California, Berkeley, California, USA.
[5]Instituto de Astronomia, Universidad Nacional Autonoma de Mexico, Mexico City, Mexico.

0148-0227/11/2011JA016559

both SIRs and CIRs are variable and the stream source strengths seem to be changing continually [*Jian et al.*, 2009, 2011].

[3] Both CIRs and SIRs are commonly bounded by forward-reverse shock pairs [e.g., *Gosling and Pizzo*, 1999]. Previous studies, using single spacecraft observations, have shown that SIR associated shocks are generally weak close to 1 AU. Since we know that the solar wind is not homogeneous, then we expect that SIR shocks structure will not be spatially uniform. In this study, one of our main objectives is to use the STEREO dual mission observation capabilities to investigate the characteristics of shocks from the same SIR observed at two different locations. We focus on shock structure and on the observed waves upstream and downstream from the shocks.

[4] A large part of our knowledge about collisionless shocks comes from studies of the Earth's bow shock, where in situ measurements are obtained much of the time. The foreshock is permeated by waves with periods of about 30 s, which can be left-hand or right-hand polarized in the spacecraft frame [see *Blanco-Cano*, 2010, and references therein]. There are also linearly polarized steepened waves, known as shocklets, which are associated with discrete wave packets [*Russell et al.*, 1971], and 1 Hz waves [*Fairfield*, 1974]. Since the speed of the solar wind relative to the spacecraft vastly exceeds the propagation speed of these shock-associated waves, the Doppler-shift by the moving solar wind plasma is important in comparing the waves at the "stationary" bow shock in comparison with the traveling interplanetary shock. This means also that to study the waves and shock structure of interplanetary shocks, a higher sampling rate is required than at the bow shock. STEREO provides this with sample rates of 8 Hz and on occasion 32 Hz.

[5] There are a few manuscripts addressing the characteristics of waves associated with interplanetary shocks. *Tsurutani and Smith* [1983] determined the properties of waves with frequencies below 3 Hz observed upstream of low Mach number (2–3) interplanetary shocks, using ISEE-3 spacecraft observations. In this study, they also found large amplitude quasiperiodic downstream waves in most of the more than 100 shocks examined. In the same way, *Russell et al.* [1983] analyzed interplanetary shocks observed by ISEE-1, ISEE-2, and ISEE-3 spacecraft in 1978 and 1979. They found two upstream waves classes: whistler mode precursors which occur at low Mach numbers, and upstream turbulence whose amplitude at Mach numbers greater than 1.5 is controlled by the angle of the field orientation to the shock normal. The former waves are right-hand circularly polarized and quite narrowband. The latter waves are more linearly polarized and have a broadband featureless spectrum. Recently, *Wilson et al.* [2007, 2009, 2010] have examined large amplitude electrostatic waves, low frequency whistler waves and shocklets associated with interplanetary shocks (with Mach numbers in the range $\sim$1–6) using high time resolution data obtained by Wind spacecraft. They found that the wave amplitude of ion acoustic waves is correlated with the fast mode Mach number and with the shock strength. *Russell et al.* [2009a], analyzed observations of low-Mach number shocks measured by STEREO and found both upstream and downstream waves. In disagreement with the prediction of early theory [see *Biskamp*, 1973], this study revealed that the downstream waves arise for a wide variety of shock conditions, and not only for $\Theta_{Bn} > 88.5°$ [see *Balikhin et al.*, 2008]. These downstream waves appear to be compressional fluctuations and may be generated by kinetic relaxation as proposed by *Ofman et al.* [2009].

[6] Traditionally, low Mach number, low plasma β shocks have been called laminar due to their well-defined structure [*Kennel et al.*, 1985]. Shock structure depends strongly on the plasma beta (β), on the angle between the shock normal and the upstream magnetic field (Θ_{Bn}), and on the upstream magnetosonic Mach number (M_{ms}) (or Alfvénic (M_A)). The M_{ms} is the ratio between the shock speed and the magnetosonic (or Alfvénic) speed, and is indicative of shock strength. As is the case for other shocks traveling in the heliosphere, SIR shocks become stronger as they move outward from the Sun. An important factor in controlling the type of shock is the direction of the upstream magnetic field relative to the shock normal. Depending on the Θ_{Bn} value, shocks are classified as quasi-parallel shocks if $\Theta_{Bn} < 45°$, and quasi-perpendicular shocks if $\Theta_{Bn} \geq 45°$.

[7] In a quasi-perpendicular shock reflected particles can not move upstream from the shock, but are transmitted downstream and a foreshock region is not expected to be formed. In contrast when $\Theta_{Bn} < 45°$, reflected protons can move upstream and a foreshock forms. In theory, laminar subcritical shocks can reach steady state through collisionless resistivity alone, and can provide dissipation through wave damping [*Kennel et al.*, 1985]. Whistler waves can phase stand in the flow while the wave energy moves upstream and damps. If the Mach number exceeds a critical value then one part of the dissipation is associated with ions that are reflected by the compressed magnetic field in the shock before being transmitted downstream. Upstream of the ramp is the foot, which is associated with the reflected ions and in which the field begins to rise from its upstream value; downstream of the ramp is the overshoot region, in which the magnetic field is larger than its downstream value by a factor which increases with Mach number. However, observations show that the transition between subcritical and supercritical shock characteristics is not as sharp as predicted by the theory. Hence, some subcritical shocks appear to be reflecting ions and develop overshoots [*Mellott and Livesey*, 1987]. Stream interaction driven interplanetary shocks are important to study since most of them are weak, sub-critical or marginally critical. Thus, by understanding their characteristics we can learn how shock physics changes from subcritical to supercritical shocks.

[8] The acceleration mechanisms occurring at highly oblique and perpendicular shocks are not yet well understood. Interplanetary quasi-parallel supercritical shocks are expected to develop a foreshock with some features similar to Earth's foreshock. The quasi-parallel orientation of the magnetic field allows reflected ions to escape upstream before being overtaken by the shock. As the reflected ions flow against the incoming plasma, they drive ion beam instabilities. These instabilities excite large amplitude waves in the upstream region forming a foreshock region. Studies of interplanetary shocks can be very useful to investigate how their foreshock structure differs from the case of planetary foreshocks. Determining foreshock waves properties and their influence on shock structure is important to

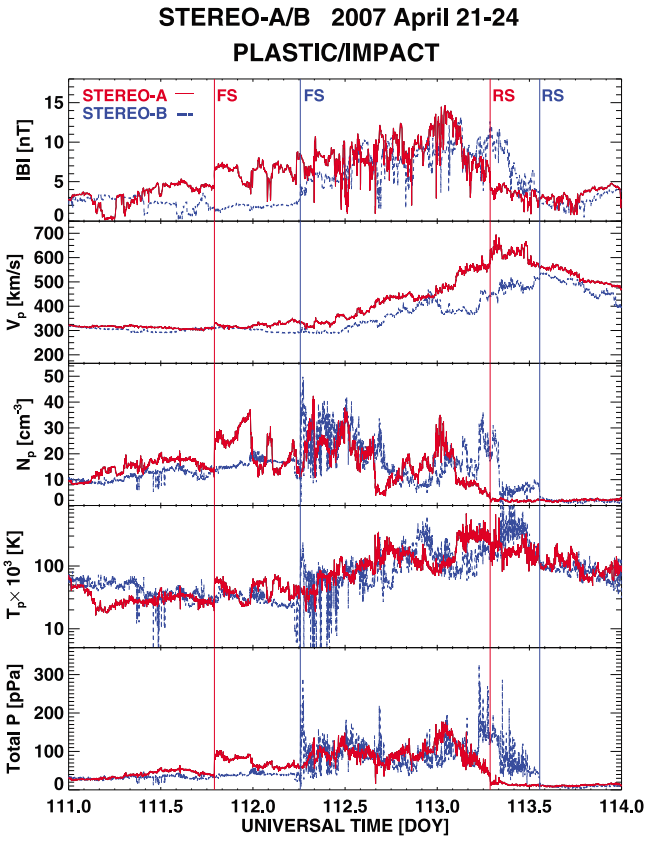

Figure 1. Forward (FS) and reverse (RS) interplanetary shocks observed by STEREO-A/B spacecraft on April 21–24, 2007. $|B|$ is the magnetic field intensity, V_p is the proton speed, N_p is the proton density, T_p is the proton temperature, and Total P is the total pressure, which represents the sum of the magnetic pressure and the perpendicular plasma (ion plus electron) thermal pressure. A constant electron temperature of 130,000 K is assumed. Due to the lack of alpha particle data, we assume its number density is 4% of the proton density, and its temperature is 4 times the proton temperature. STEREO magnetic field and plasma data are plotted at a resolution of 1 minute each.

enhance our understanding of acceleration processes at these shocks.

[9] Since the launch of the STEREO mission at the end of 2006, a considerable number of interplanetary shocks have been detected by both spacecraft. Because the Sun was at its minimum phase, there are very few events related to interplanetary coronal mass ejections (ICMEs), and the majority of interplanetary shocks during 2007–2008 are associated with SIRs. The high resolution provided by STEREO magnetic field data has allowed us to identify waves of different types in the vicinity of SIR associated shocks. *Jian et al.* [2009] have studied three 2007 SIRs in detail and demonstrated the variability of SIRs and their associated shocks. They found that these investigated shocks are still in development at 1 AU. In this work we investigate the characteristics of 9 interplanetary shocks associated with SIRs observed by both STEREO-A and STEREO-B spacecraft during the years 2007–2008. The complete list of stream interaction shocks is available at: http://www-ssc.igpp.ucla.edu/forms/stereo/stereo_evel_3.html. The comparison of dual observations of SIR associated shocks allow us to get insight in SIR evolution and changes in shock structure, strength, and orientation. Moreover, these changes in shock structure are important for the type of waves that can be generated in the upstream and downstream shock regions. In this work we provide these observations.

2. Observations and Analysis

[10] The IMPACT (In situ Measurements of Particles And CME Transients) investigation [*Luhmann et al.*, 2008] on the STEREO mission [*Kaiser et al.*, 2008] provides multipoint solar wind and suprathermal electron, interplanetary magnetic field, and solar energetic particle measurements. The magnetic field instrument (IMPACT-MAG) [*Acuña et al.*, 2008] on board each STEREO spacecraft returns vector field measurements at 8 Hz and 32 Hz. STEREO also carries The Plasma and Suprathermal Ion Composition (PLASTIC) investigation that returns solar wind moments with 1 minute time resolution [*Galvin et al.*, 2008]. These instruments are used to identify SIRs based on the following criteria [*Jian et al.*, 2006]: (1) an increase of solar wind speed, (2) a pile-up of total perpendicular pressure (P_t) with gradual decreases at both sides from the P_t peak to the edges of the interaction region, (3) bulk flow velocity deflections, (4) an increase and then decrease of proton number density (N_p), (5) an enhancement of proton temperature T_p), (6) an increase of the entropy defined as $ln(T_p^{3/2}/N_p)$ [*Siscoe and Intriligator*, 1993; *Crooker et al.*, 1996], and (7) a compression of the magnetic field. In their classification of stream interactions *Jian et al.* [2006] required that the variations in the solar wind must satisfy at least 5 of the criteria to be classified as a SIR.

[11] The forward and reverse shocks are identified using 8-Hz magnetic field data. At forward shocks, the solar wind speed, proton number density, proton temperature, and magnetic field should increase simultaneously. At reverse shocks, solar wind speed increases, while proton number density, proton temperature, and magnetic field all decrease. We rotated these data into shock normal coordinates to examine the properties of associated shock waves and field changes. The magnetosonic Mach number (M_{ms}) is obtained from Rankine-Hugoniot equations using magnetic field and solar wind moments measurements at 1-minute resolution.

[12] Figure 1 shows plasma data from STEREO/PLASTIC and magnetic field data from STEREO/IMPACT for April 21–24, 2007 within an example of an observed stream interaction region. Both spacecraft observed two interplanetary shocks during this period of time, corresponding to the forward and reverse SIR shocks. On April 21 STEREO-A observed a well developed forward quasi-perpendicular ($\Theta_{Bn} = 77°$) shock. The sharp jump in the quasi-perpendicular shock is in contrast to the more gradual and fluctuating quasi-parallel ($\Theta_{Bn} = 40°$) shock observed by STEREO-B on April 22, ~11 hours later. The Mach number for the forward shock was lower at STEREO-A ($M_{ms} = 1.40$) than STEREO-B ($M_{ms} = 1.81$). On April 23 STEREO-A observed a well developed reverse quasi-perpendicular ($\Theta_{Bn} = 73°$) shock, while STEREO-B observed a reverse quasi-parallel ($\Theta_{Bn} = 34°$) shock, ~6 hours later. The Mach number for the

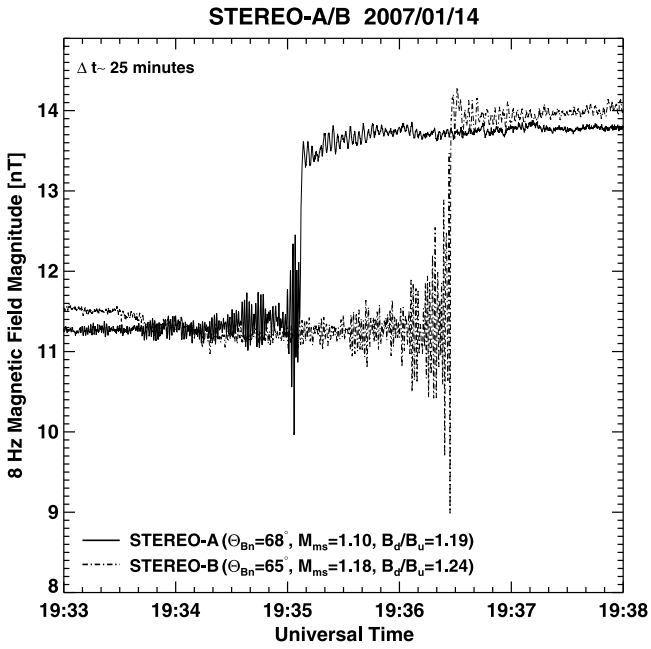

Figure 2. Weak quasi-perpendicular forward shock observed by STEREO-A/B on January 14, 2007. The time in STEREO-A remains fixed while in STEREO-B is shifted by $\Delta t \sim 25$ min backward. This shock crossed STEREO-B $\sim$ 26 min later than STEREO-A. The separation angle between the spacecraft was $\sim$0.3° on the ecliptic plane. As a consequence of this small separation, the shock structure is qualitatively the same at the two locations, and the shock wave normal angle, Mach number, and field jump are also similar for both shocks.

reverse shock was lower at STEREO-A (M_{ms} = 1.22) than STEREO-B (M_{ms} = 2.12).

[13] High time-resolution (8 Hz, and 32 Hz when available) magnetic field data just upstream and downstream of all 9 shock pairs (18 single shocks) analyzed were examined to determine the presence (or absence) of waves and their characteristics. We found that low frequency waves were detected upstream and downstream of almost all the shocks examined. Upstream from the shocks, whistlers, low frequency waves ($f \leq 1$ Hz), and some broadband-low-frequency fluctuations are observed. There are two shocks where foot and overshoot signatures are observed. No waves were found upstream from one shock, another one shows a few whistlers observed by STEREO-A and no clear waves in STEREO-B. Downstream from the shocks there are whistlers, low frequency waves, and low frequency fluctuations.

2.1. Weak Quasi-Perpendicular Shock

[14] On January 14, 2007 a weak stream interaction shock crossed STEREO-A at 19:35:08 UT. This quasi-perpendicular forward shock crossed STEREO-B $\sim$26 min later than STEREO-A. The separation angle in the ecliptic plane between the spacecraft was $\sim$0.3°. Figure 2 shows a 5-minute time window where both shocks are observed. The time in STEREO-A remains fixed while in STEREO-B is shifted backwards in time by $\Delta t \sim 25$ min in order to compare this shock at the two different locations. Qualitatively the shock structure is the same at the two locations. The shock wave normal angle, Mach number, and field jump are similar for both shocks: Θ_{Bn} = 68° and 65°; M_{ms} = 1.10 and 1.18; B_d/B_u = 1.19 and 1.24, for STEREO-A and STEREO-B, respectively.

[15] Figure 3 shows a 1-minute zoom, using 32-Hz magnetic field data, of the stream interaction shock observed by STEREO-A and shown in Figure 2. This higher resolution allows us to see in greater detail the magnetic field variations than do the lower resolution data at 8 Hz. No 32-Hz data were available for STEREO-B for this shock. As can be seen in Figure 3, the whistler waves upstream of the shock observed by STEREO-A appear as trains of different amplitude with the largest amplitude train observed just before the shock transition. No overshoot is observed, and downstream the waves do not appear as trains of different amplitude. We use minimum variance analysis (MVA) [*Sonnerup and Scheible*, 1998], and fast Fourier transform (FFT) to analyze wave properties. Basically our analysis starts with an inspection, using 8 Hz (or 32 Hz) magnetic field data in radial-tangential-normal (RTN) coordinates, of the upstream and downstream regions very close (few minutes) to each shock. If a wave pattern (magnetic field oscillations) is observed then we apply a FFT analysis in order to identify wave power at various frequencies to see which frequencies are contributing to the fluctuations. Moreover, our FFT analysis computes transverse and compressive powers for a better contrast and characterization of the waves. The compressive power is defined from the total power P_{tot}, which is the result of applying FFT to the total magnetic field $|B|$, while the transversal power is defined as

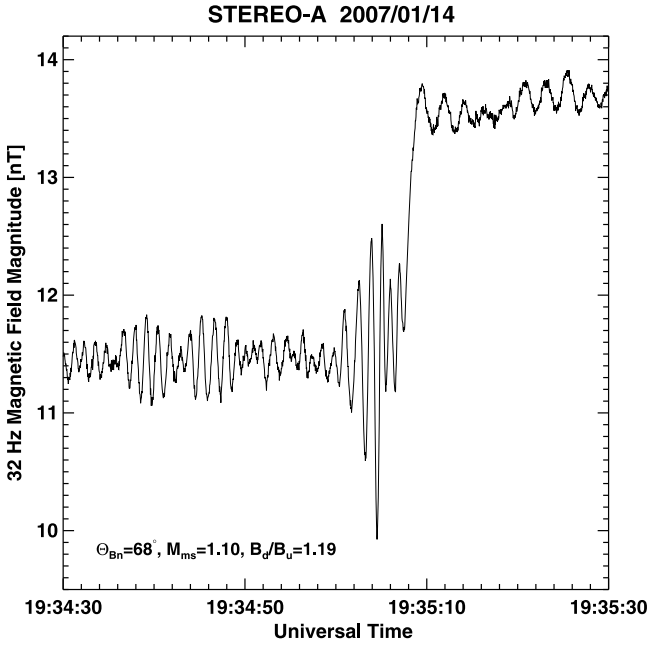

Figure 3. One-minute zoom of the weak quasi-perpendicular forward shock, shown in Figure 2, observed by STEREO-A on January 14, 2007. Magnetic field data are at 32-Hz resolution which allows us to see in more detail the magnetic field variations upstream and downstream from the shock.

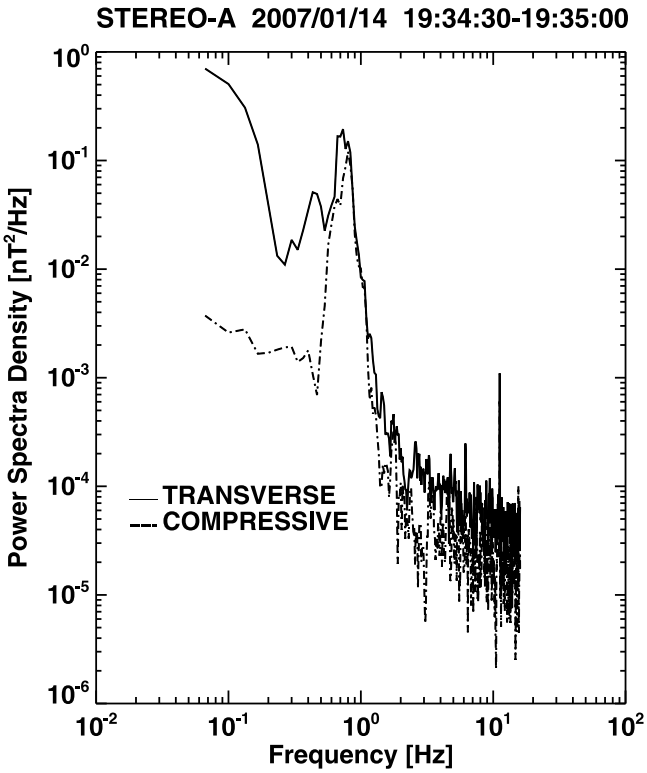

Figure 4. Power spectral density upstream from the weak quasi-perpendicular forward shock shown in Figure 3, observed by STEREO-A on January 14, 2007, with 32-Hz magnetic field data resolution. The transverse and compressive powers show a main peak around ~0.9 Hz.

$|P_r + P_t + P_n - P_{tot}|$, where P_r, P_t, P_n, are the fluctuating wave power along the magnetic field components B_r, B_t and B_n. Wave propagation angles ($\Theta_{B_o k}$ and Θ_{nk}) and polarization properties are obtained by applying MVA. We find that whistler precursors are observed with frequencies around 0.9 Hz (STEREO-A) and 0.15 Hz (STEREO-B). Figure 4 shows the FFT analysis applied on a 30-second interval of time (19:34:30–19:35:00 UT), using 32-Hz magnetic field data, just before the shock crossed STEREO-A. In this case, the compressive (dash-dotted line) and the transversal (solid line) powers have similar values, showing a main peak around ~0.9 Hz. In the same way, using MVA over five specific time intervals, we find that these whistler waves propagate at angles ranging from $\Theta_{B_o k} = 25°$ to $\Theta_{B_o k} = 59°$ (STEREO-A), and from $\Theta_{B_o k} = 28°$ to $\Theta_{B_o k} = 41°$ (STEREO-B), with respect to the ambient magnetic field. Their angle of propagation with respect to the shock normal, for the same five time intervals, ranges from $\Theta_{nk} = 18°$ to $\Theta_{nk} = 42$ (STEREO-A), and from $\Theta_{nk} = 38°$ to $\Theta_{nk} = 43°$ (STEREO-B). Compressive waves can also exist downstream from these shocks for a variety of shock conditions [*Russell et al.*, 2009b]. Downstream from this shock compressive waves are observed with frequencies around 0.6 Hz in both STEREO-A/B spacecraft. These waves propagate at angles which range from $\Theta_{B_o k} = 28°$ to $\Theta_{B_o k} = 67$ (STEREO-A), and from $\Theta_{B_o k} = 1°$ to $\Theta_{B_o k} = 5°$, with respect to the ambient magnetic field. Their angle of propagation with respect to the shock normal ranges from $\Theta_{nk} = 28°$ to $\Theta_{nk} = 47°$ (STEREO-A), and from $\Theta_{nk} = 65°$ to $\Theta_{nk} = 71°$ (STEREO-B).

2.2. Strong Quasi-Perpendicular Shock

[16] Figure 5 shows a quasi-perpendicular shock observed by both STEREO-B (November 19, 2007) and STEREO-A (November 20, 2007) spacecraft. The separation angle between the spacecraft was ~40.8°. The shock observed by STEREO-B is stronger ($M_{ms} = 1.84$) compared with STEREO-A ($M_{ms} = 1.18$). Plasma β and B_d/B_u values are also higher in STEREO-B ($\beta = 2.34$; $B_d/B_u = 1.84$) compared with STEREO-A ($\beta = 1.14$; $B_d/B_u = 1.12$). When the M_{ms} increases, the interplanetary shock profile changes and starts to develop foot and overshoot regions, which are common signatures of supercritical shocks. This explains why the magnetic field intensity profile observed by STEREO-B shows a foot and an overshoot region, which are associated with ion reflection and gyration, while the lower plasma β and M_{ms} shock observed by STEREO-A does not.

[17] Both shocks also show whistler precursors in the upstream region. On STEREO-A whistler precursors appear during a very short time interval and their amplitude is small while in STEREO-B these precursors are superposed on the foot region. Upstream from the shock whistler precursors are observed with frequencies around 0.9 Hz (STEREO-A) and 2 Hz (STEREO-B). These waves propagate at angles that range from $\Theta_{B_o k} = 2°$ to $\Theta_{B_o k} = 12°$ (STEREO-A), and from $\Theta_{B_o k} = 22°$ to $\Theta_{B_o k} = 31°$ (STEREO-B), with respect to the ambient magnetic field. Their angle of propagation with respect to the shock normal ranges from $\Theta_{nk} = 62°$ to $\Theta_{nk} = 76°$ (STEREO-A), and from $\Theta_{nk} = 29°$ to $\Theta_{nk} = 38°$

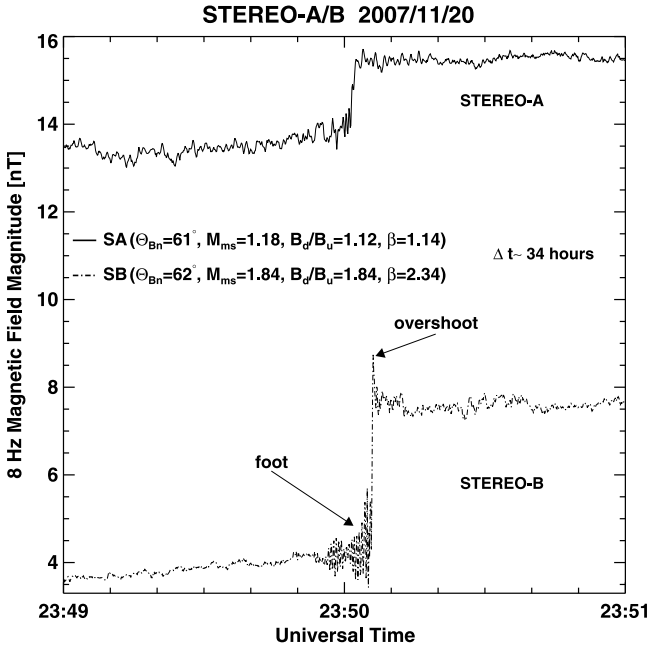

Figure 5. Strong quasi-perpendicular forward shock observed by STEREO-A/B on November 19–20, 2007. The time in STEREO-A remains fixed while in STEREO-B is shifted by Δt ~34 hours forward. The shock observed by STEREO-B shows foot and overshoot regions, which are common signatures in supercritical shocks.

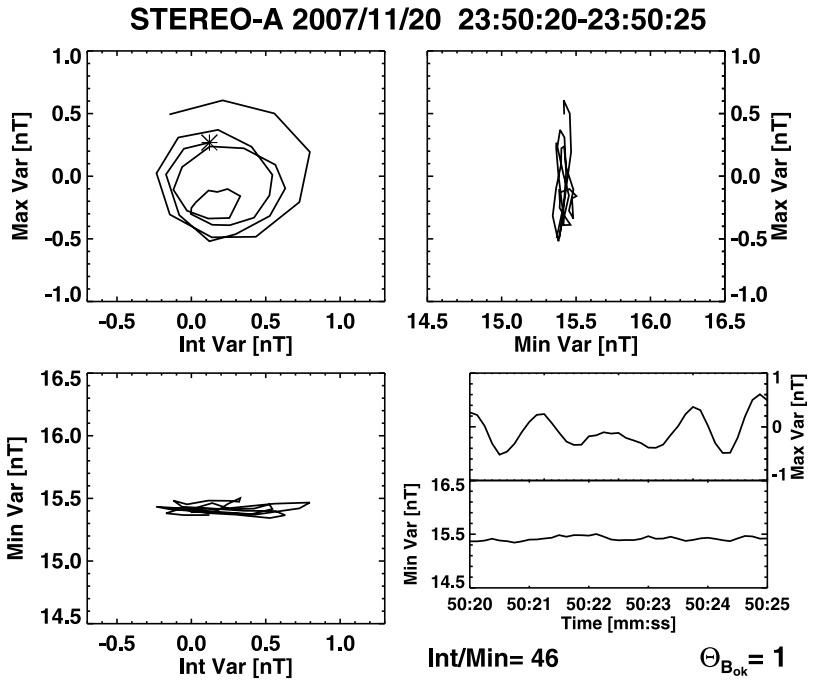

Figure 6. Magnetic field hodograms obtained by the MVA performed on a 5-second interval of time (23:50:20–23:50:25) downstream from the shock observed by STEREO-A on November 20, 2007, where whistler waves were observed. These waves are right-hand circularly polarized in the spacecraft frame and propagate at an angle of ∼1° to the magnetic field, with a frequency around 0.1 Hz (see Table 1). The intermediate to minimum eigenvalue ratio is ∼46. The asterisk indicates the beginning of the interval.

(STEREO-B). The large values of Θ_{nk} for the upstream precursors suggest that they are not phase standing waves. These fluctuations are similar to the waves found by *Wilson et al.* [2009] who explain their origin in terms of electron instabilities. In the downstream region STEREO-A observed whistlers with frequencies around 0.1 Hz while in STEREO-B waves are observed with frequencies around 0.4 Hz. These waves propagate at angles which range from $\Theta_{B_o k} = 1°$ to $\Theta_{B_o k} = 14°$ (STEREO-A), and from $\Theta_{B_o k} = 2°$ to $\Theta_{B_o k} = 20°$ (STEREO-B), with respect to the ambient magnetic field. Their angle of propagation with respect to the shock normal ranges from $\Theta_{nk} = 62°$ to $\Theta_{nk} = 78°$ (STEREO-A), and from $\Theta_{nk} = 56°$ to $\Theta_{nk} = 89°$ (STEREO-B). Figure 6 shows the MVA analysis performed on a 5-second interval where whistler waves were observed downstream from the shock at STEREO-A. We can notice that these waves are right-hand circularly polarized in the spacecraft frame.

[18] Table 1 summarizes shock parameters and the upstream and downstream waves analysis of the 9 shocks associated with SIRs that were observed by both spacecraft. According to Table 1, upstream from shock fronts whistler waves, low frequency waves, and some broadband-low-frequency fluctuations are observed in most of the events with frequencies ranging from ∼0.15 up to ∼2 Hz. The average values for the angles $\Theta_{B_o k}$ and Θ_{nk} are ∼25°, and ∼51°, respectively, which tell us that these upstream waves propagate on average at quasi-parallel angles with respect to the magnetic field, and at quasi-perpendicular angles with respect to the shock normal. Two shocks (numbers 6 and 9) also show foot and overshoot regions on STEREO-B crossings. Downstream from shock fronts whistler waves, low frequency waves, and fluctuations with frequencies ranging from ∼0.2 up to ∼1.5 Hz, are observed. The average values in our set of events are $\Theta_{B_o k} \sim 35°$, and $\Theta_{nk} \sim 58°$. Hence, as in the upstream regions, these downstream waves propagate on average at quasi-parallel angles with respect to the magnetic field, and at quasi-perpendicular angles with respect to the shock normal, respectively. The shock number 4, observed by STEREO-A, also shows mirror mode waves in the downstream region [see *Russell et al.*, 2009b].

3. Solar Wind Conditions

[19] The plasma and magnetic field conditions upstream from shock fronts play an important role in determining whether or not we see similar shocks on STEREO-A/B. We would expect that the plasma parameters change significantly while both spacecraft are drifting apart, i.e., if we see similar shocks on STEREO-A/B it is because the plasma parameters also look the same in their surrounding regions, while at greater separations the plasma parameters could show more variations and we would see different characteristics in the stream interaction region observed by the two spacecraft. However, the analysis of the nine events used in this work shows that shock parameters are different at the two locations, but there is not a general trend to conclude that parameters are increasingly different as longitudinal separation increases. It is possible that our data set is not sufficiently large to see a clear trend.

[20] Table 2 shows average magnetic field ($|B|$) and plasma (N_p and T_p) values (used to compute plasma β)

Table 1. Shock Parameters and the Upstream and Downstream Wave Analysis Corresponding to 9 Shocks Associated With SIRs Observed by Both STEREO-A and STEREO-B Spacecraft[a]

Number and Shock Type	Spacecraft and Shock Date/Time	B_d/B_u	Θ_{Bn}	β	M_{ms}	Upstream			Downstream		
						Waves	$\Theta_{B_o k}$	Θ_{nk}	Waves	$\Theta_{B_o k}$	Θ_{nk}
01-F	SA 07/01/14 19:35:08	1.19	68	DG	1.10	whistlers $f \sim 0.9$ Hz	59	18	whistler $f \sim 0.6$ Hz	63	65
	SB 07/01/14 20:01:27	1.24	65	DG	1.18	whistlers $f \sim 0.15$ Hz	38	43	whistler $f \sim 0.6$ Hz	1	69
02-F	SA 07/04/21 18:59:15	1.57	77	3.91	1.40	whistlers $f \sim 2$ Hz	14	63	whistler $f \sim 0.2$ Hz	76	159
	SB 07/04/22 06:09:27	1.58	40	5.70	1.81	low frequency waves $f \sim 0.6$ Hz	5	39	fluctuations $f \sim 0.7$ Hz	23	52
03-R	SA 07/04/23 06:53:44	1.32	73	1.67	1.22	fluctuations $f \sim 0.3$ Hz	17	73	fluctuations $f \sim 0.3$ Hz	6	72
	SB 07/04/23 13:21:10	1.65	34	4.32	2.12	low frequency waves $f \sim 0.15$ Hz	27	42	fluctuations $f \sim 0.2$ Hz	37	70
04-F	SA 07/05/07 08:11:54	1.72	80	4.35	1.53	few whistlers $f \sim 2$ Hz	49	32	whistlers and mirror mode waves, $f \sim 1$ Hz	45	40
	SB 07/05/07 09:42:49	1.65	63	2.24	1.55	no clear waves	–	–	whistlers $f \sim 1.5$ Hz	78	151
05-F	SA 07/05/22 01:59:45	1.21	47	0.96	1.20	small whistlers $f \sim 0.5$ Hz	83	80	few whistlers $f \sim 1.5$ Hz	67	44
	SB 07/05/22 17:29:52	1.33	81	0.24	1.25	fluctuations $f \sim 0.8$ Hz	3	81	whistlers $f \sim 1.5$ Hz	8	81
06-R	SA 07/07/11 20:22:25	2.25	62	1.04	2.20	no clear waves	–	–	whistlers $f \sim 0.4$ Hz	77	17
	SB 07/07/11 07:44:44	1.97	63	0.94	1.83	whistlers, $f \sim 0.8$ Hz, foot and overshoot in shock	43	20	no clear waves	–	–
07-R	SA 07/09/30 11:09:06	1.55	77	0.30	1.42	fluctuations $f \sim 0.5$ Hz	2	79	whistlers $f \sim 0.7$ Hz	16	70
	SB 07/09/29 07:54:21	1.87	41	1.96	2.20	small whistlers $f \sim 1.5$ Hz	2	47	fluctuations $f \sim 0.7$ Hz	38	72
08-F	SA 07/11/20 23:50:02	1.12	61	1.14	1.18	whistlers $f \sim 0.9$ Hz	2	62	whistlers $f \sim 0.1$ Hz	1	66
	SB 07/11/19 13:49:36	1.84	62	2.34	1.84	whistlers, $f \sim 2$ Hz, foot and overshoot in shock	22	36	low frequency waves $f \sim 0.4$ Hz	15	89
09-F	SA 08/12/06 05:42:30	1.42	45	7.50	1.50	low frequency waves $f \sim 1$ Hz	32	76	low frequency waves $f \sim 0.4$ Hz	20	39
	SB 08/12/07 04:35:30	1.44	20	DG	1.98	whistlers $f \sim 0.4$ Hz	4	22	whistlers $f \sim 0.2$ Hz	29	21

[a]Column 1 shows the event number and shock type (forward (F) or reverse (R)). Column 2 shows the spacecraft (STEREO-A or STEREO-B), date (yy/mm/dd) and time (hh:mm:ss) of the shocks as they crossed each spacecraft. Column 3 is the ratio of downstream magnetic field intensity to upstream magnetic field intensity (B_d/B_u). Column 4 shows the shock normal angle Θ_{Bn}. Column 5 is the ratio of the plasma pressure to the magnetic pressure (plasma β), where DG indicates a data gap. Columns 6 shows the magnetosonic Mach number (M_{ms}). Columns 7–12 show the results of the wave analysis we applied in order to determine the type of waves observed and their properties (upstream and downstream from the shocks), where $\Theta_{B_o k}$ is the angle at which the waves propagate with respect to the ambient magnetic field, and Θ_{nk} is the angle at which waves propagate with respect to the shock normal.

corresponding to all upstream regions from shock fronts observed by both spacecraft. Moreover, we also added average plasma β, B_d/B_u, and M_{ms} values. We can notice that, on average, the magnetic field, the proton density, and the proton temperature values are higher in STEREO-A compared to STEREO-B, which tell us about the different plasma conditions each spacecraft encounters at different locations.

[21] The plasma β was quite variable between STEREO-A and STEREO-B independent of their separation (see Table 1). Plasma conditions reveal marked differences at the time the shock crossed each spacecraft (see Figure 7). In the case of the shock observed by STEREO-A the average values (upstream from shock front) of $|B|$, N_p, and T_p were 13.41 nT, 19.64 cm^{-3}, and 4.8×10^4 K, respectively. On the other hand, plasma conditions for the shock observed by STEREO-B were $|B| = 3.71$ nT, $N_p = 9.63$ cm^{-3}, and $T_p = 5.3 \times 10^4$ K. This indicates that STEREO-A was in a location where magnetic field and density were higher compared with STEREO-B. However, the temperature at STEREO-B was higher than that at STEREO-A at the moment the shock crossed it.

[22] Figure 8 shows the spacecraft location with the Parker's spiral overplotted for the shock number 8 (see Figure 5). The approximate distance between STEREO-A and STEREO-B is $\sim 106 \times 10^6$ km ($\sim$0.7 AU). The black arrows represent the shock normal at each spacecraft, while the solid bars represent the shock front at each location. This

Table 2. Average $|B|$, N_p, T_p, Plasma β, B_d/B_u, and M_{ms} Corresponding to 9 Shocks Associated With SIRs Observed by Both STEREO-A and STEREO-B Spacecraft

	$\|B\|$ (nT)	N_p (cm^{-3})	T_p (K)	Plasma β	B_d/B_u	M_{ms}
SA	7.4	10.5	8.4×10^4	2.6	1.5	1.4
SB	5.3	6.5	5.7×10^4	2.5	1.5	1.75
Average	6.35	8.5	7.1×10^4	2.55	1.5	1.58

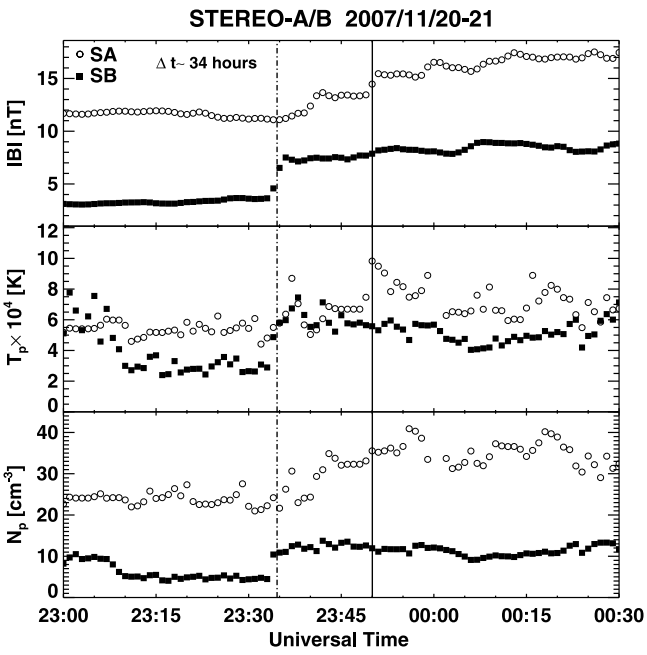

Figure 7. One-minute resolution plasma parameters of the shock number 8 observed by STEREO-A/B on November 19–20, 2007. The solid line shows the time where the shock crossed STEREO-A (open circles), and the dash-dotted line shows the time where the shock crossed STEREO-B (filled squares). The time in STEREO-A remains fixed while the time in STEREO-B is shifted by Δt ~34 hours forward. The parameters for the shock observed by STEREO-A are Θ_{Bn} = 61°, M_{ms} = 1.18, B_d/B_u = 1.12, while those for the shock observed by STEREO-B are Θ_{Bn} = 62°, M_{ms} = 1.84, B_d/B_u = 1.84.

spatial scale of the SIR shock tells us how the shock characteristics change basically with longitude, which is also reflected in the downstream region observed by each spacecraft (see Figure 7). M_{ms} is lower in STEREO-A (1.18) compared to STEREO-B (1.84), which is related, as we have seen, to the inhomogeneity in the solar wind stream characteristics that are present in the heliosphere.

4. Summary

[23] Interplanetary shocks are complex structures surrounded by regions where a variety of wave modes exist. STEREO dual observations show that the characteristics of a shock can change dramatically from one region to another in both the upstream and downstream regions. As STEREO-A and STEREO-B drift apart, the shocks that they see occur in different solar wind conditions. So they should see different upstream fields and plasma conditions. We find that the variations with longitude of shock parameters do not vary more as the spacecraft separation increases, they just vary without following a trend. This may be due to the fact that our data set is not sufficiently large to see a clear trend.

[24] We analyzed 9 shocks associated with stream interaction regions (SIRs) observed by both STEREO-A and STEREO-B spacecraft during the years 2007–2008, when the Sun was at its solar minimum phase of activity. These events took place during a very low solar activity phase where the interplanetary medium is dominated mainly by recurrent high-speed streams coming from polar, midlatitude large scale, and low latitude small scale coronal holes [e.g., *Kilpua et al.*, 2009]. This sample of events considers only shocks that were observed by both spacecraft, and no other selection criteria was used. For this study the separation angle between the spacecraft was in the range ~0.2° to ~86°. We found that both spacecraft observed shocks with a wide variety of Θ_{Bn} (range: [~20° to ~81°]), shock magnetosonic Mach number (range: [~1.1 to ~2.2]), and field jump (range: [~1.1 to ~2.25]) values. The largest changes for Θ_{Bn}, shock magnetosonic Mach number, and field jump, at the two different longitudinal locations, were ~39°, ~0.9, and ~0.72, respectively.

[25] Our study shows that the upstream and downstream regions associated with shocks can be permeated by different types of waves and that low Mach number shocks are much more complex structures than originally thought [see also *Wilson et al.*, 2007, 2009, 2010]. Upstream from shock fronts whistler and low frequency, likely beam generated (associated with quasi-parallel shocks) waves were present. Downstream from shock fronts whistler waves and compressive fluctuations, including mirror modes were found. Further work, including the study of ion and electron distributions, is needed to determine exactly the origin of each type of wave and the microphysics that determines the characteristics of interplanetary shocks and their surrounding regions. The large angles of propagation with respect to shock normal found for the whistler precursors indicates that they are not phase standing waves. These fluctuations resemble the waves found by *Wilson et al.* [2009] whose origin has been attributed to electron kinetic instabilities

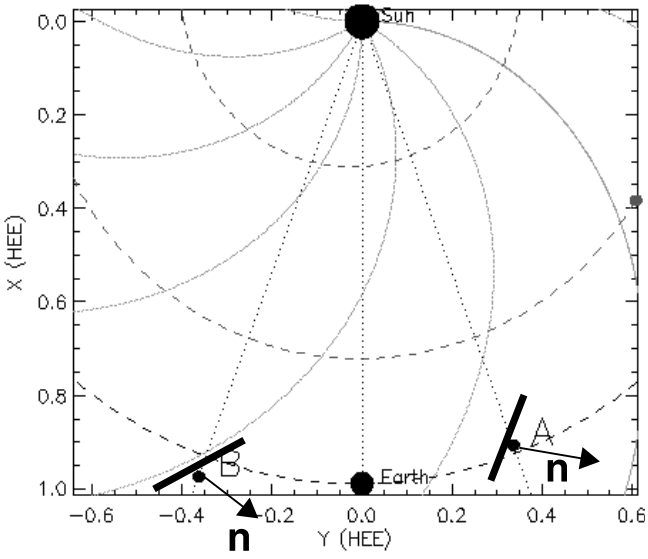

Figure 8. Spacecraft location with the Parker's spiral overplotted for the shock number 8 observed by STEREO-A/B on November 19–20, 2007. The black arrows represent the shock normal at each spacecraft, while the solid bars represent the shock front at each location. The axes on the plot are in the Heliocentric-Earth-Ecliptic (HEE) coordinate system, where X is the Sun-Earth line in astronomical units (AU), and Z points to the north pole.

such as the whistler heat flux and/or the whistler anisotropy instabilities. On the other hand, the existence of a foot and overshoot for some of the shocks indicates that ion reflection is taking place so that some of the low frequency waves observed further upstream may be generated by ion instabilities such as the right-hand resonant instability via cyclotron resonance. For the interplanetary shocks where ion reflection is taking place we expect foreshock regions filled with suprathermal ions upstream from these shocks, where wave particle interactions take place modifying both wave and particle distributions characteristics. Examining in more detail wave particle interactions near interplanetary shocks will enhance our understanding about how thermalization takes place in these shocks and will give us insight about acceleration processes.

[26] A recent study has shown, by analyzing dynamic energy spectra from the STEREO-PLASTIC ion spectrometer, that ICME driven shocks can have very long (many hours) foreshock regions with suprathermal ions in contrast to the stream interaction shocks that show much smaller heated regions upstream (X. Blanco-Cano et al., manuscript in preparation, 2011). This suggests that ICME driven shocks have been in existence longer, almost all the way from the Sun, whereas the stream interaction shocks analyzed in this work have only been in existence a short time before being observed at 1 AU. Hence, the ICME shocks would have heated protons and generated upstream waves over a long distance and the integral/average foreshock would depend on the average shock structure from the Sun to STEREO which might be quite different than the local structure. For stream interactions this would be less true since the near-shock upstream waves and hot particle distributions are more related to the shock seen at STEREO because that structure has just recently been formed.

[27] **Acknowledgments.** We thank the reviewers for their constructive comments to improve this manuscript. E. Aguilar-Rodriguez thanks DGAPA-PAPIIT project (grant IN110309-2) and CONACyT project (grant 101625). X. Blanco-Cano thanks CONACyT project (grant 81154). C. T. Russell's and L. K. Jian's research is supported by the NASA STEREO program through Grant NAS5-03131 administered by UC Berkeley.

[28] Philippa Browning thanks the reviewers for their assistance in evaluating this paper.

References

Acuña, M. H., D. Curtis, J. L. Scheifele, C. T. Russell, P. Schroeder, A. Szabo, and J. G. Luhmann (2008), The STEREO/IMPACT magnetic field experiment, *Space Sci. Rev.*, *136*, 203–206, doi:10.1007/s11214-007-9259-2.

Arge, C. N., and V. J. Pizzo (2000), Improvement in the prediction of solar wind conditions using near-real time solar magnetic field updates, *J. Geophys. Res.*, *105* , 10,465–10,479.

Balikhin, M. A., T. L. Zhang, M. Gedalin, N. Y. Ganushkina, and S. A. Pope (2008), Venus Express observes a new type of shock with pure kinematic relaxation, *Geophys. Res. Lett.*, *35*, L01103, doi:10.1029/2007GL032495.

Biskamp, D. (1973), Collisionless shock waves in plasmas, *Nucl. Fusion*, *13*, 719–740.

Blanco-Cano, X. (2010), Bow shocks in the solar wind: Lessons towards understanding interplanetary shocks, *AIP Conf. Proc.*, *1216*, 459–465.

Crooker, N. U., M. E. Burton, G. L. Siscoe, S. W. Kahler, J. T. Gosling, and E. J. Smith (1996), Solar wind streamer belt structure, *J. Geophys. Res.*, *101*, 24,331–24,341.

Fairfield, D. H. (1974), Whistler waves observed upstream from collisionless shocks, *J. Geophys. Res.*, *79*, 1368–1378.

Feldman, W. C., J. R. Asbridge, S. J. Bame, E. E. Fenimore, and J. T. Gosling (1981), The solar origins of solar wind interstream flows: Near-equatorial coronal streamers, *J. Geophys. Res.*, *86*(A7), 5408–5416.

Galvin, A. B., et al. (2008), The Plasma and Suprathermal Ion Composition (PLASTIC) investigation on the STEREO observatories, *Space Sci. Rev.*, *136*, 437–486, doi:10.1007/s11214-007-9296-x.

Gosling, J. T., and V. J. Pizzo (1999), Formation and evolution of corotating interaction regions and their three dimensional structure, *Space Sci. Rev.*, *89*, 21–52.

Gosling, J. T., J. R. Asbridge, S. J. Bame, W. C. Feldman, G. Borrini, and R. T. Hansen (1981), Coronal streamers in the solar wind at 1 AU, *J. Geophys. Res.*, *86*, 5438–5448.

Gosling, J. T., et al. (2001), Stream interaction regions at high heliographic latitudes during Ulysses' second polar orbit, *Space Sci. Rev.*, *67*, 189–192.

Jian, L. K., C. T. Russell, J. G. Luhmann, and R. M. Skoug (2006), Properties of stream interactions at one AU during 1995–2004, *Sol. Phys.*, *239*, 337, doi:10.1007/s11207-006-0132-3.

Jian, L. K., C. T. Russell, J. G. Luhmann, A. B. Galvin, and P. J. MacNeice (2009), Multi-spacecraft observations: Stream interactions and associated structures, *Sol. Phys.*, *259*, 345–360, doi:10.1007/s11207-009-9445-3.

Jian, L. K., C. T. Russell, J. G. Luhmann, P. J. MacNeice, D. Odstrcil, P. Riley, J. A. Linker, R. M. Skoug, and J. T. Steinberg (2011), Comparison of observations at ACE and Ulysses with Enlil model results: Stream interaction regions during Carrington rotations 2016–2018, *Sol. Phys.*, doi:10.1007/s11207-011-9858-7, in press.

Kaiser, M. L., T. A. Kucera, J. M. Davila, O. C. St. Cyr, M. Guhathakurta, and E. Christian (2008), The STEREO mission: An introduction, *Space Sci. Rev.*, *136*, 5–16, doi:10.1007/s11214-007-9296-x.

Kennel, C. F., J. P. Edmiston, and T. Hada (1985), A quarter century of collisionless shock research, in *Collisionless Shocks in the Heliosphere: A Tutorial Review*, *Geophys. Monogr. Ser.*, vol. 34, edited by R. G. Stone and B. T. Tsurutani, pp. 1–36, AGU, Washington, D. C.

Kilpua, E. K. J., et al. (2009), Small solar wind transients and their connection to the large-scale coronal structure, *Sol. Phys.*, *256*(1–2), 327–344.

Krieger, A. S., A. F. Timothy, and E. C. Roelof (1973), A coronal hole and its identification as the source of a high velocity solar wind stream, *Sol. Phys.*, *29*, 505–525.

Luhmann, J. G., et al. (2008), STEREO IMPACT investigation goals, measurements, and data products overview, *Space Sci. Rev.*, *136*, 117–184.

Mellott, M. M., and W. A. Livesey (1987), Shock overshoots revisited, *J. Geophys. Res.*, *92*, 13,661–13,665.

Ofman, L., M. Balikhin, C. T. Russell, and M. Gedalin (2009), Collisionless relaxation of ion distributions downstream of laminar quasi-perpendicular shocks, *J. Geophys. Res.*, *114*, A09106, doi:10.1029/2009JA014365.

Russell, C. T., D. D. Childers, and J. P. J. Coleman (1971), OGO 5 observations of upstream waves in interplanetary medium: Discrete wave packets, *J. Geophys. Res.*, *76*, 845–861.

Russell, C. T., E. J. Smith, B. T. Tsurutani, J. T. Gosling, and S. J. Bame (1983), Multiple spacecraft observations of interplanetary shocks: Characteristics of the upstream ULF turbulence, in *Solar Wind Five*, edited by M. Neugebauer, *NASA Conf. Publ., CP-2280*, 385–400.

Russell, C. T., L. K. Jian, X. Blanco-Cano, and J. G. Luhmann (2009a), STEREO observations of upstream and downstream waves at low Mach number shocks, *Geophys. Res. Lett.*, *36*, L03106, doi:10.1029/2008GL036991.

Russell, C. T., X. Blanco-Cano, L. K. Jian, and J. G. Luhmann (2009b), Mirror-mode storms: STEREO observations of protracted generation of small amplitude waves, *Geophys. Res. Lett.*, *36*, L05106, doi:10.1029/2008GL037113.

Sheeley, N. R., T. N. Knudson, and Y.-M. Wang (2001), Coronal inflows and the Sun's nonaxisymmetric open flux, *Astrophys. J.*, *546*, L131–L135.

Siscoe, G., and D. Intriligator (1993), Three views of two giant streams: Aligned observations at 1 AU, 4.6 AU, and 5.9 AU, *Geophys. Res. Lett.*, *20*(20), 2267–2270.

Sonnerup, B. U. Ö., and M. Scheible (1998), Minimum and maximum variance analysis, in *Analysis and Methods for Multi-spacecraft Data*, edited by G. Paschmann and W. Daly, *Sci. Rep., SR-001*, pp. 185–220, Eur. Space Agency, Noordwijk, Netherlands.

Tsurutani, B. T., and E. J. Smith (1983), Waves observed upstream of interplanetary shocks, *J. Geophys. Res.*, *88*, 5645–5656.

Wang, Y.-M., N. R. Sheeley, D. G. Socker, R. A. Howard, and N. B. Rich (2000), The dynamical nature of coronal streamers, *J. Geophys. Res.*, *105*, 25,133–25,142.

Wilson, L. B., III, et al. (2007), Waves in interplanetary shocks: A Wind/WAVES study, *Phys. Rev. Lett.*, *99*, 041101.

Wilson, L. B., III, C. A. Cattell, P. J. Kellogg, K. Goetz, K. Kersten, J. C. Kasper, A. Szabo, and K. Meziane (2009), Low-frequency whistler

waves and shocklets observed at quasi-perpendicular interplanetary shocks, *J. Geophys. Res.*, *114*, A10106, doi:10.1029/2009JA014376.

Wilson, L. B., III, C. A. Cattell, P. J. Kellogg, K. Goetz, K. Kersten, J. C. Kasper, A. Szabo, and M. Wilber (2010), Large-amplitude electrostatic waves observed at a supercritical interplanetary shock, *J. Geophys. Res.*, *115*, A12104, doi:10.1029/2010JA015332.

E. Aguilar-Rodriguez, Unidad Michoacan, Instituto de Geofisica, Universidad Nacional Autonoma de Mexico, Morelia, Michoacan 58098, Mexico. (ernesto@geofisica.unam.mx).

X. Blanco-Cano, Instituto de Geofisica, Universidad Nacional Autonoma de Mexico, Mexico City 04510, Mexico.

L. K. Jian and C. T. Russell, Institute of Geophysics and Planetary Physics, University of California, Los Angeles, CA 90095, USA.

J. G. Luhmann, Space Sciences Laboratory, University of California, Berkeley, CA 94720, USA.

J. C. Ramírez Vélez, Instituto de Astronomia, Universidad Nacional Autonoma de Mexico, Mexico City 04510, Mexico.